Cleaner Engineering and Technology 15 (2023) 100660

Contents lists available at ScienceDirect

Cleaner Engineering and Technology

journal homepage: www.sciencedirect.com/journal/cleaner-engineering-and-technology

Microwave-assisted green synthesis of silver nanoparticles using pineapple leaves waste

Siti Nor Syairah Anis [a], Wen Ching Liew [a], Aishah Mohd Marsin [b], Ida Idayu Muhamad [a,c,*], Sin Hui Teh [a], Ahmad Zahran Md Khudzari [c]

[a] Department of Bioprocess & Polymer Engineering, Faculty of Chemical and Energy Engineering, Universiti Teknologi Malaysia, UTM, 81310, Johor Bahru, Johor, Malaysia
[b] Kolej Komuniti Pasir Salak, Jalan Lebuh Paduka, Changkat Lada, 36800, Kampung Gajah, Perak, Malaysia
[c] IJN-UTM Cardiovasular Engineering Centre, Institute of Human Centered Engineering, Universiti Teknologi Malaysia, UTM, 81310, Johor Bahru, Johor, Malaysia

ARTICLE INFO

Keywords:
silver nanoparticles
Microwave-assisted
Green synthesis
Leaves extract
Antimicrobial
Ananas comosus

ABSTRACT

A cost-effective and eco-friendly method for synthesizing silver nanoparticles using pineapple leaves waste mediated by microwave-assisted extraction is presented. The green synthesis of AgNPs is accomplished through a simple reduction method utilizing silver nitrate. Various parameters, including silver nitrate concentration (5–25 mM), incubation time (2–24 h), and sample volume (2–8 mL), are employed to determine the optimal green synthesis condition. The presence of an absorption band in the range of 400–500 nm in the UV–Vis spectrophotometer indicates the reduction of silver metal ions into silver nanoparticles. The intensity of the absorption is found to increase with prolonged duration and higher concentrations of the silver nitrate solution and sample volume. FE-SEM results demonstrate that the green synthesized silver nanoparticles range in size from 40 to 150 nm and display hexagonal spherical-shaped structures. Furthermore, FTIR and XRD analyses confirm the presence of green synthesized AgNPs. The microwave-assisted treatment of silver nanoparticles exhibits greater antimicrobial activity against *Escherichia coli*, *Bacillus subtilis*, and *Staphylococcus aureus* compared to non-microwave-assisted treatment. The minimum inhibitory concentration of silver nanoparticles for bacterial growth is 60 μg/mL. Overall, this research offers a promising avenue for the eco-friendly and cost-effective green synthesis of silver nanoparticles using the microwave-assisted method, with significant potential in various applications.

1. Introduction

The field of nanotechnology is a cutting-edge area of science that has numerous applications across a range of industries, including energy, industrial production, and biomedical research (Lin et al., 2009; Madkour, 2019; Sabbagh et al., 2021). By engineering nanoparticles (NPs) with unique compositions and functionalities, nanotechnology offers new techniques that were not previously possible in biomedical research. The numerous potentials, advantages, and applications of nanotechnology in biology and biomedical research cannot be ignored (Wang and Wang, 2014). Among NPs, silver nanoparticles (AgNPs) have recently been found to have strong inhibitory and antibacterial properties, making them a hot topic in various fields including biomedical device coatings, food packaging, cosmetics, water purification, and even as therapeutic agents (Emeka et al., 2014; Wang and Wang, 2014; Nithya and Vimala, 2014; Ren et al., 2019; Al-Askar et al., 2013). The unique characteristic of AgNPs, which have a size range between 1 and 100 nm, have attracted interest owing to their properties such as electrical, optical and magnetic features that provide a wide range of applications (Galatage et al., 2021). AgNPs are also capable of reducing microbial infections in skin and wounds and inhibiting bacterial colonization on different surfaces of devices (Wang and Wang, 2014).

AgNPs can be produced using either physical or chemical methods, but these traditional methods are costly and have environmental concerns due to the production of harmful by-products and the utilization of toxic chemicals. The importance of green synthesis of AgNPs lies in its environmentally friendly approach, which minimizes the potential risks posed by traditional chemical or physical synthesis methods. This makes

* Corresponding author. Department of Bioprocess & Polymer Engineering, Faculty of Chemial and Energy Engineering, Universiti Teknologi Malaysia, UTM 81310 JohorBahru, Johor, Malaysia.
E-mail address: idaidayu@utm.my (I.I. Muhamad).

https://doi.org/10.1016/j.clet.2023.100660
Received 18 February 2023; Received in revised form 24 June 2023; Accepted 13 July 2023
Available online 15 July 2023

it a crucial aspect in ensuring the sustainability and safe application of AgNPs in various fields. With this concern, non-hazardous and green synthesis methods for synthesizing colloidal AgNPs have been currently developed, such as through the use of microorganisms or plants (Nagalingam et al., 2018). Plant-mediated synthesis is becoming a preferred method due to its advantages such as being non-toxic, eco--friendly, and cost-effective compared to microorganisms which require aseptic condition for cell culture (Wang and Wang, 2014; Al-Askar et al., 2013; Nagalingam et al., 2018). Plants, containing biomolecule compounds such as proteins, flavonoids, polyphenols, and other phytochemicals, serve as capping and reducing agents for AgNP synthesis (Wang and Wang, 2014; Al-Askar et al., 2013). The resulting particles are stable and come in various sizes and shapes. Furthermore, microwave-assisted green synthesis of AgNPs is noteworthy since it has been reviewed to offer several advantages across various fields and can be readily utilized in different size as well as structure (Kaur et al., 2022).

Different plants have been used for AgNP synthesis, including *Aegle marmelos* (Wang and Wang, 2014), *Pteris tripartite* (Al-Askar et al., 2013), *Prosopis farcta* (Baskaran et al., 2016), *Acalypha indica* (Priyadarshini et al., 2013), *Curcuma longa* (Salari et al., 2019), *Ananas comosus* (Chawalitsakunchai et al., 2021; Hamdiani and Shih, 2021) and many more. *A. comosus* or pineapple is a major fruit crop in Malaysia, along with papaya, pomelo, banana, watermelon, jackfruit, and mango. The production of pineapple generates a significant amount of waste, including stems, crowns, cores, and peels, with as much as 30–50% of the total fruit weight discarded during canning. Currently, 95% of the canned pineapple produced in Malaysia is for export, with the remaining 5% for domestic consumption (Krishnaraj et al., 2010). A waste-to-wealth initiative has been proposed to convert this waste into something useful to reduce the amount of waste. This study demonstrates that the waste from the MD2 "Super Sweet" pineapple leaves can serve as a capping and reducing agent for the green synthesis of AgNPs using a microwave-assisted method, and has potential for antibacterial applications in various fields. The novelty of this study lies in the application of microwave-assisted method, which is more energy-saving compared to traditional energy-consuming heating method (Emeka et al., 2014; Hamdiani and Shih, 2021) for the reduction of Ag^{+} ion to Ag^{0}. This innovative procedure offers greener and more time effective advantages in term of energy consumption.

2. Methodology

2.1. Materials

Silver nitrate ($AgNO_3$) was procured from RCI Labscan Limited, Bangkok, Thailand. Pineapple leave waste was collected from pineapple plantation industry in Johor.

2.2. Preparation of pineapple leaf waste extract

The wasted pineapple leaves are thoroughly washed several times with running tap water to remove dust and then rinsed with distilled water. The air-dried leaves are cut into small pieces, and approximately 100 g are weighed. These leaves are then boiled in 400 mL of distilled water at 100 °C for 30 min and filtered. Part of the filtrate is used as a reducing agent and stabilizer for the green synthesis of AgNPs. The filtrate is stored at −20 °C to prevent contamination of the aqueous plant extract. The residual leaves from the filtrate are dried in an oven until they reached a constant weight and blended for FTIR analysis as a control.

2.3. Green synthesis of AgNPs

The green synthesis of AgNPs is performed using aqueous extraction from wasted pineapple leaves through a simple reduction method with

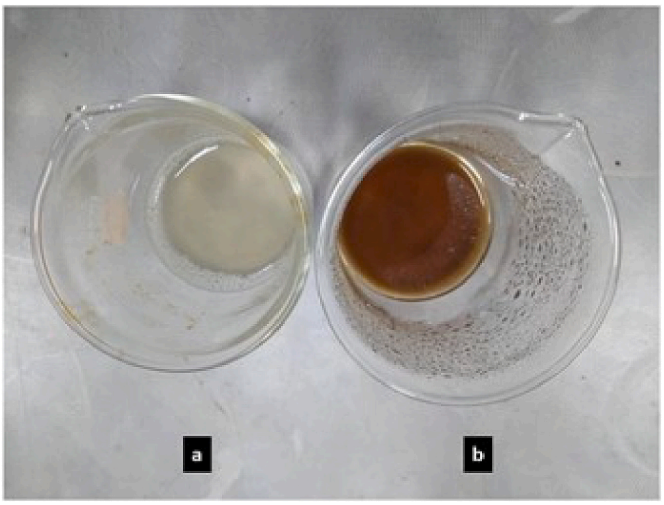

Fig. 1. Colour of aqueous solution (a) before added $AgNO_3$ and (b) after added $AgNO_3$ under microwave-assisted treatment. (For interpretation of the references to colour in this figure legend, the reader is referred to the Web version of this article.)

$AgNO_3$. The green synthesis process is done in accordance to Kumar et al. (2021) with slight modifications. To begin, 20 mM of $AgNO_3$ solution is added to 4 mL of the pineapple leaves extract solution in a total volume of 20 mL, with stirring. The solution is then incubated at room temperature. The green synthesis is conducted by comparing microwave-assisted treatment with normal condition. The microwave-assisted treatment is performed at a constant power of 10% x 1100 Watts for 9 min. Upon completion, the colour of aqueous extract changes from colourless to reddish brown slowly when adding $AgNO_3$. The rapid formation of a reddish-brown solution, as shown in Fig. 1, indicates the successful formation of AgNPs through the reduction of silver ions in the solution. The green synthesized AgNPs are then purified by washing twice with distilled water, centrifuging (using MPW-352R, Germany) at 8000 rpm for 10 min, and lyophilizing using a freeze drier machine (Alpha 1-2 LDplus, Martin Christ, Germany). Different parameters include $AgNO_3$ concentration (5–25 mM), incubation time (2–24 h) and sample volume (2–8 mL) are further studied to determine the optimal condition for synthesizing AgNPs.

2.4. Characterization of AgNPs

2.4.1. UV–vis spectrophotometer

The UV–Vis microplate spectrophotometer reader (Epoch microplate spectrophotometer, US) is used to initially characterize the green-synthesized AgNPs, which involves the reduction of pure silver ions. The surface plasmon absorption in the range of 350–600 nm of wavelength is recorded.

2.4.2. Field-Emission Scanning Electron Microscopy (FESEM)

The prepared gold coated samples are characterized under FESEM (ZEISS, Crossbeam 340, Germany) to observe the morphological characterization of green synthesized AgNPs.

2.4.3. Fourier Transform Infrared (FTIR)

The leaves left after extraction and the green synthesized AgNPs are analyzed using a FTIR spectrophotometer at a range of 4,000 to 400 cm^{-1} (Perkin- Elmer Spectrum One FT-IR Spectrometer, USA).

2.4.4. X-Ray Diffractometer (XRD)

X-ray diffraction (XRD) is performed on the powdered AgNP samples using a Shimadzu XRD-6000 instrument from Japan. The size of the AgNPs is determined by drop-coating them onto glass substrates, and the

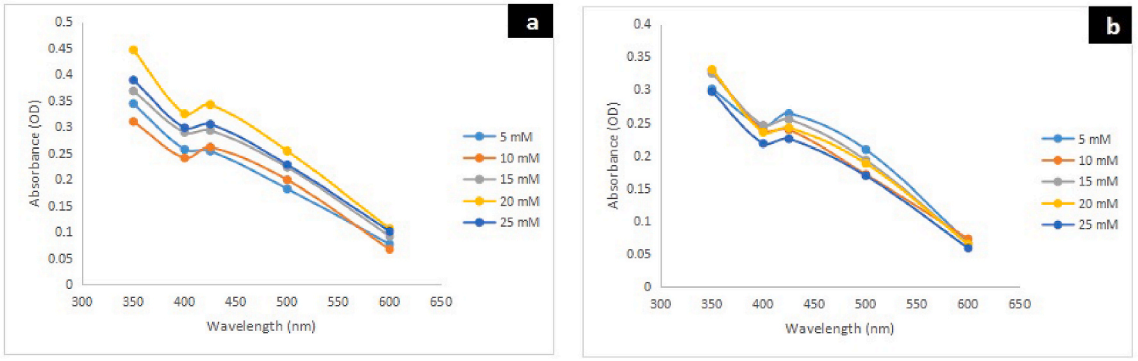

Fig. 2. Effect of different $AgNO_3$ concentration on green synthesized AgNPs for (a) Microwave-assisted treatment; (b) Normal condition. (For interpretation of the references to colour in this figure legend, the reader is referred to the Web version of this article.)

presence of AgNPs is confirmed by assaying the dried mixture after the water has evaporated at room temperature. The XRD analysis is conducted using Cu Kα radiation in a θ to 2θ configuration, with a voltage of 40 kV and a current of 30 mA.

2.5. Antimicrobial activity

2.5.1. Microbial culture

Three bacteria are collected from ATCC 6538. The bacterial strains included Gram-negative bacteria, *E. coli* and Gram-positive bacteria, *B. subtilis* and *S. aureus*. *S. aureus* is chosen as delegate as the most

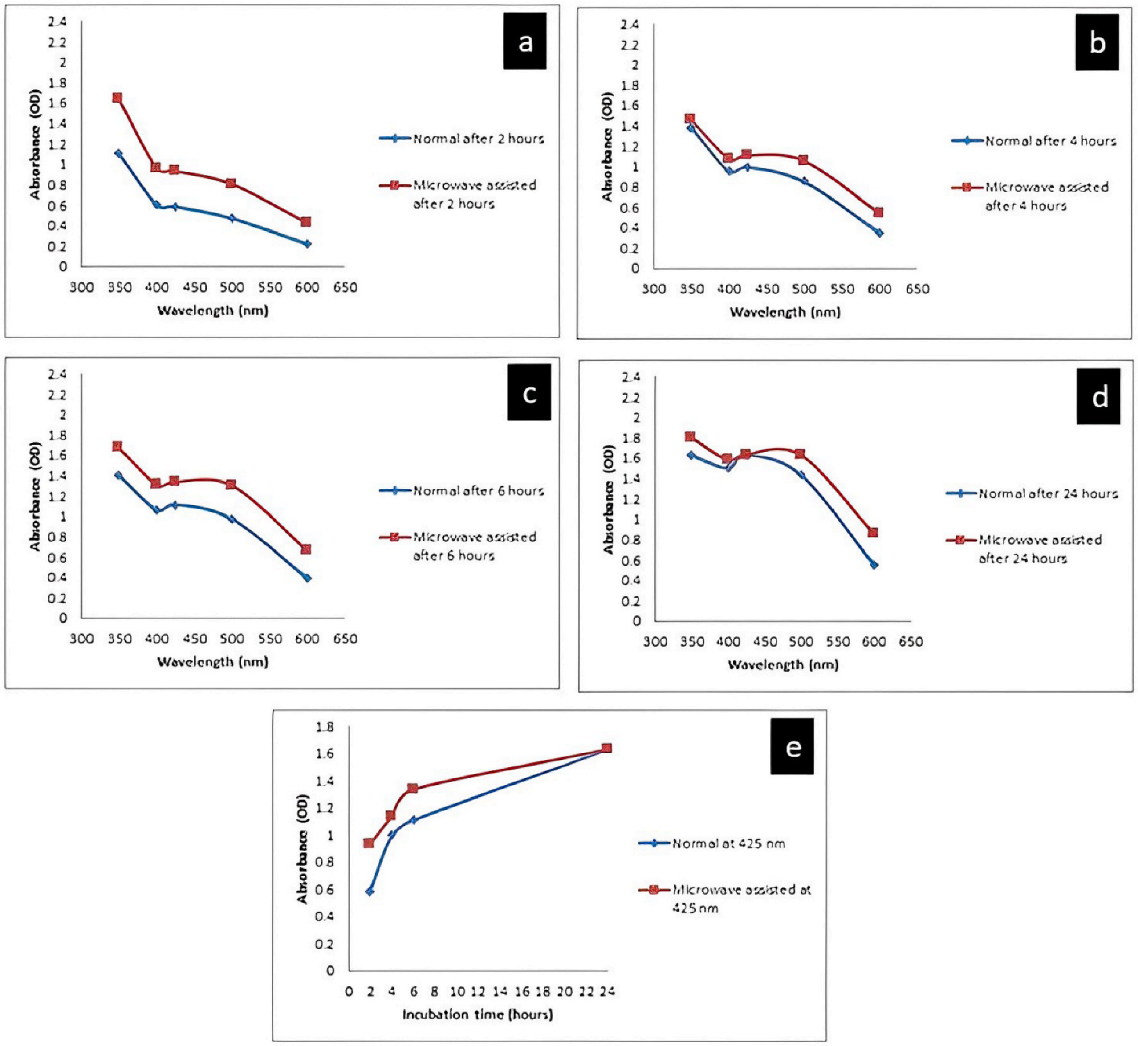

Fig. 3. Effect of different incubation time on green synthesized AgNPs under (a) 2hr; (b) 4 h; (c) 6 h; (d) 24 h of incubation time; (e) wavelength comparison between normal condition and microwave-assisted treatment at 425 nm. (For interpretation of the references to colour in this figure legend, the reader is referred to the Web version of this article.)

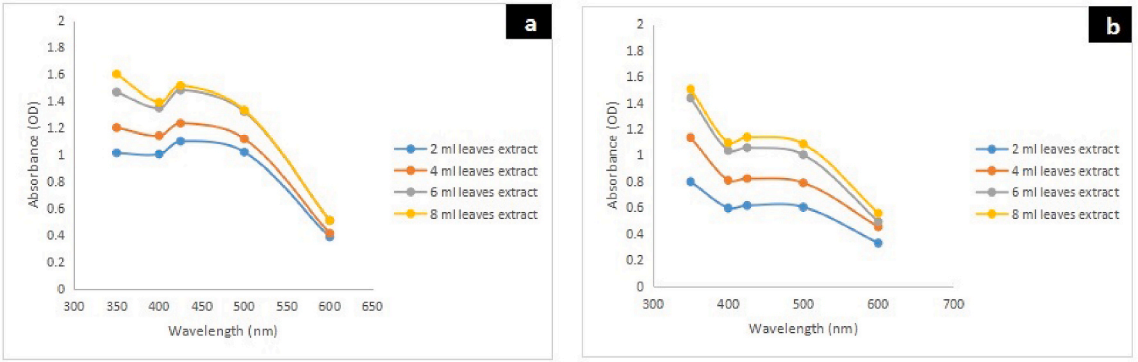

Fig. 4. Effect of different sample volume of extraction wasted pineapple leaves for (a) microwave-assisted treatment; (b) normal condition.

common infection bacteria in wound.

2.5.2. Disk diffusion antibacterial assay

Disk diffusion antimicrobial assay was done according to Baskaran et al. (2016). The process of creating agar plates involves pouring 20 mL of sterile nutrient agar liquid into a sterile Petri dish and spreading 0.1 mL of bacterial suspension over the nutrient agar plates after solidification. Sterile filter paper disks (6 mm in diameter) were impregnated with 5 and 10 μL of 5 mg/mL of AgNPs and then incubated the plates at 37 °C for 24 h. Antibacterial activity was assessed by measuring the zones of inhibition against the test microorganisms.

2.5.3. Broth antibacterial assay

Simultaneously, 1 mL of three type bacterial suspension in nutrient broth (NB) is transfer into 15 mL NB in universal bottle with different concentration of green synthesized AgNPs. The bacterial suspensions are incubated for 24 h. After 24 h, the bacterial growth is determined by dry cell weight calculation obtained by optical density (OD) reading at 600 nm using spectrophotometer (UV-1280 spectrophotometer, Shimadzu, Japan) (Alsamhary, 2020).

3. Results and discussion

3.1. Optimal condition for green synthesis of AgNPs

Green synthesis of AgNPs using wasted pineapple leaves extract is potentially advantageous compare to other methods since it is easy to improve, less biohazardous, and free from toxic chemicals. Additionally, it provides natural capping agents for the stabilization of silver nanoparticles and is more cost-competitive compared to nanoparticle synthesis by microorganisms (Ahmed et al., 2016). Green synthesis of AgNPs involves collecting wasted pineapple leaves, washing them thoroughly with running water (necrotic plants and epiphytes were removed), washing again with sterile distilled water (associated debris were removed), cutting them into small pieces, boiling them in distilled water, and filtering the extract. The synthesis of AgNPs involves utilizing a portion of the filtrate from the boiled and filtered pineapple leaves extract as a reducing agent and stabilizer. The reaction occurred during the addition of $AgNO_3$ solution into a few volumes of plant extract under microwave-assisted treatment or normal treatment condition. Several parameter were investigated in this study and the reduction of pure Ag (I) ions to Ag(0) were monitored by measuring under UV–vis spectrophotometry microplate reader of the solution at regular interval (Kumar et al. (2021).

3.1.1. Effect of different $AgNO_3$ concentration

Effect of different $AgNO_3$ concentration (ranging from 5 to 25 mM) is examined to determine the optimal concentration of $AgNO_3$ to reduce the silver ion for green synthesized AgNPs in 4 mL leaves extract solution. Different wavelengths in UV–vis spectrophotometry microplate reader are shown the highest peak ranges between 400 and 450 nm at different concentrations of $AgNO_3$ during green synthesis of AgNPs for 2 h incubation period as demonstrated in Fig. 2. Similar UV spectrum range was reported by Mojally et al. (2022) using aqueous mint extract and Lade and Patil (2022) using leaves extract of *Passiflora foetida Linn*. The collective oscillations of conduction electrons in nanoparticles in the presence of visible light give rise to the Surface Plasmon Resonance (SPR) band, which is strongly affected by the size and shape of the nanoparticles. The AgNPs produced from the pineapple leaves extract exhibited a reddish-brown color when suspended in water, which can be attributed to the excitation of electrons and changes in electronic energy levels caused by the reduction of Ag^{+} into Ag^{0} (Emeka et al., 2014). Fig. 2a shows that the green synthesis performs increase intensity with the higher of peaks at 20 mM of $AgNO_3$ for 2 h of incubation time with microwave-assisted treatment. This implies that the concentration of 20 mM $AgNO_3$ is sufficient to reduce the silver ion for green synthesized AgNPs as compare to others concentration. The band at 400-450 becoming high as increase the concentration because the number of organic compounds absorption is increasing (Ramya, 2021). However, as the concentration further increase to 25 mM, the SPR intensity decreases. This phenomenon may be owing to the restricted accessibility of active functional groups present in the pomelo peels extract to function as reducing agents. Conversely, no significant difference is shown in the normal condition (Fig. 2b) as slower reaction of reduction of silver ion occurs without treatment with microwave.

3.1.2. Effect of different incubation time

The effect of different incubation time (2, 4, 6, 24 h of incubation) on green synthesized AgNPs with normal condition and microwave-assisted treatment at 20 mM $AgNO_3$ and 4 mL extract leaves is examined as shown in Fig. 3. The intensity UV–Vis spectra of the absorption increase with distinctive plasmon band ranging between 400 and 450 nm with prolong time incubation, indicating the formation of the AgNPs increased by continuous incubation until 24 h. During the initial incubation, the SPR peak was observed at approximately 401 nm, which gradually shifted towards longer wavelengths with the increase in reaction time. The intensity of the SPR peak was observed to increase with an increase in reaction time, suggesting a higher concentration of the synthesized AgNPs. The enhancement in SPR intensity could potentially be attributed to the conversion of hydroxyl (OH) groups to carbonyl (C=O) groups as a result of the reduction of silver ions, as suggested by Jalani et al. (2018). Fig. 3e depicts the comparison of green synthesis AgNPs by normal condition with microwave-assisted treatment with different incubation time at 425 nm. Green synthesis of AgNPs by microwave-assisted treatment accelerates more formation of AgNPs during 2–6 h of incubation as compared with green synthesis in normal condition. The formation of AgNPs achieves same intensity after 24 h of incubation and the graph intensity becomes flatter, representing a

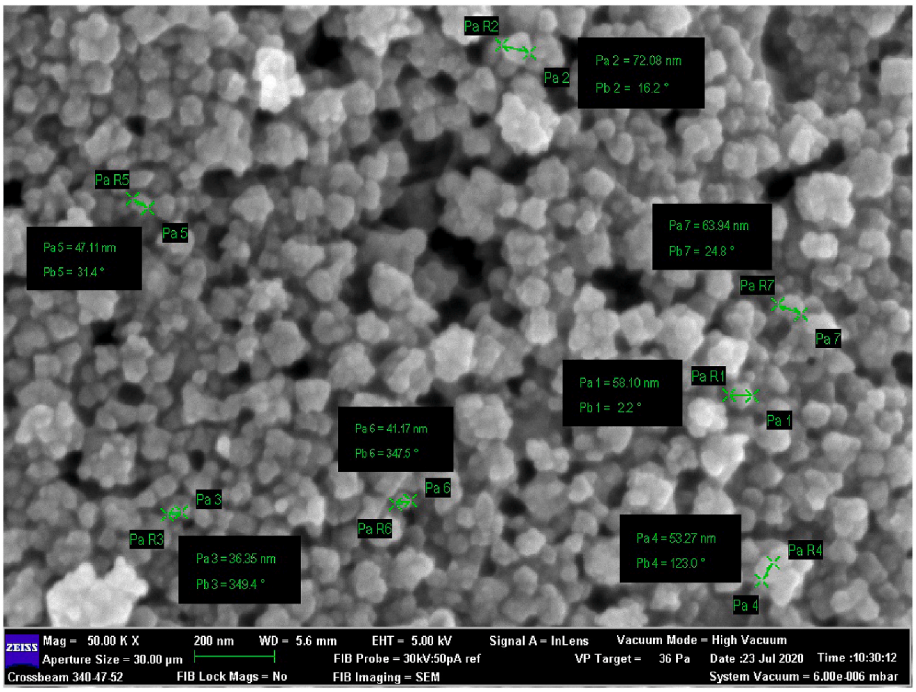

Fig. 5. The particle size and morphology of AgNPs under FESEM 50 000 x magnification.

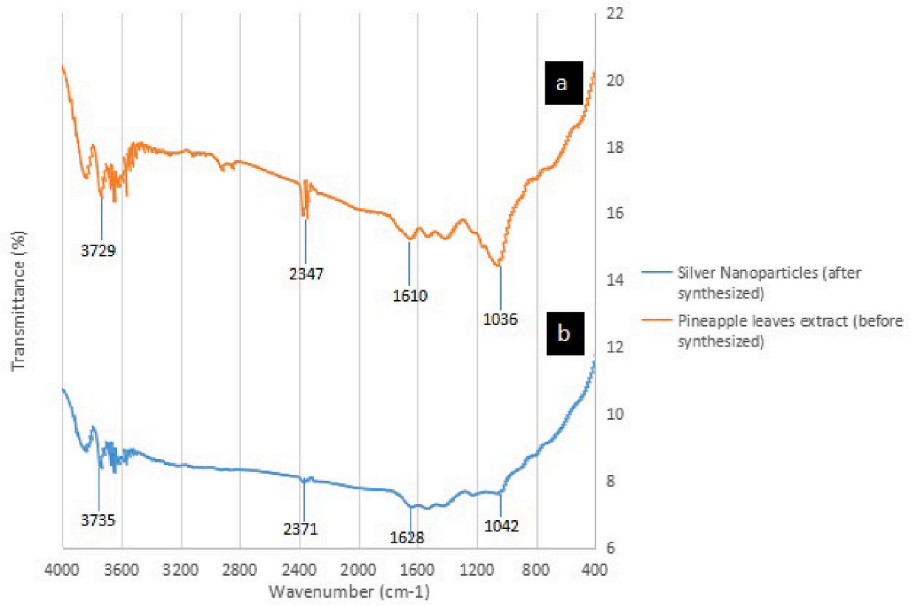

Fig. 6. FTIR absorbance spectra of control (residual leaves filtrated), A-leaves extract (before synthesized) and B- AgNPs (after synthesized).

completion of AgNPs formation in the reaction suspension.

3.1.3. *Effect of different sample volume*

Different sample volumes (2, 4, 6, 8 mL) of extracted wasted pineapple leaves are employed in green synthesis under 6 h incubation. The peaks are observed in the range of 400–450 nm as shown in Fig. 4 for both experiment with and without microwave-assisted treatment. Both results reveal that 6 mL and 8 mL sample volume of leaves extract are sufficient for the reaction with 20 mM $AgNO_3$. This is because the highest wavelength was performed by 6 mL and 8 mL, indicating faster reduction activity of silver ion. It is in line with the study done by Jyothi et al. (2022) where 8 mL of *Spondias pinnata* bark extract was the optimal amount of AgNPs synthesis by microwave irradiation as the SPR band changed with different volume. Therefore, AgNPs synthesized from the treatment of 20 mM of $AgNO_3$ using 6 mL sample volume with microwave-assisted treatment for 6 h of incubation time was employed for further characterization analysis.

3.2. *Characterization of AgNPs*

3.2.1. *Particle size and morphology*

Fig. 5 illustrates the morphology and particle size of AgNPs synthesized using microwave-assisted method. The nanoparticles are observed to have a hexagonal spherical shape, with a size range between 40 and 150 nm. The size of AgNPs is slightly larger than that in the work by Maryani and Septama (2022) (21.63 ± 4.85 nm) and Jyothi et al. (2022)

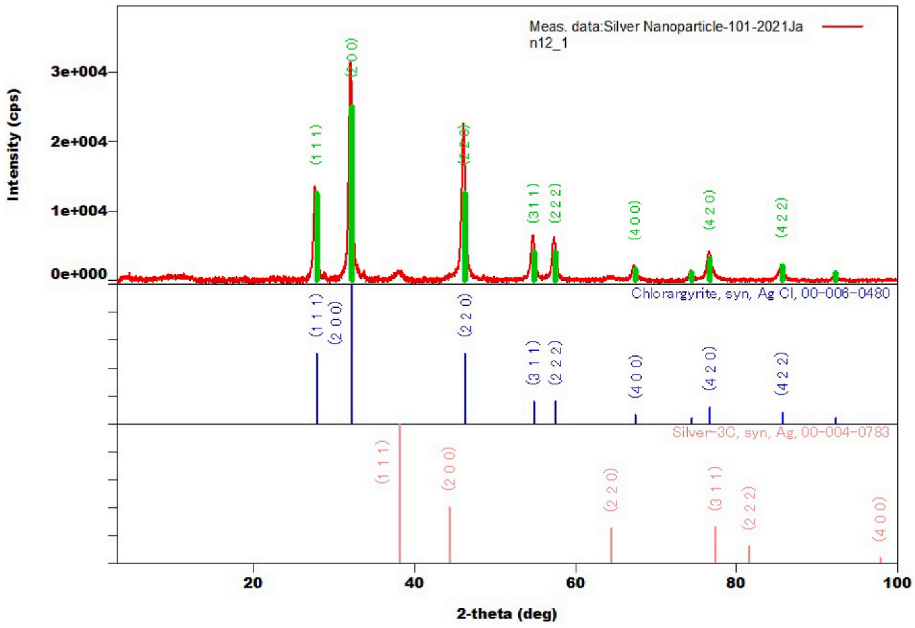

Fig. 7. XRD pattern for green synthesized AgNP using microwave-assisted treatment. (For interpretation of the references to colour in this figure legend, the reader is referred to the Web version of this article.)

(34.52 nm). Researchers claimed that smaller size could perform better antimicrobial activity since it can penetrate to bacterial cells easily thereby disrupting their cell wall (Arshad et al., 2021). Moreover, spherical size of AgNPs demonstrates a larger specific surface area compared to nanorods and nanowires (Acharya et al., 2018) thus can inhibit the antimicrobial growth more effectively through penetration and reaction with bacterial cell wall.

3.2.2. FTIR analysis

Functional groups in samples can be examined with FTIR spectroscopy in order to verify the efficacy of each step of the treatment. Fig. 6 depicts FTIR spectra of pineapple leaves; A - pineapple leaves extract and B - AgNPs. The comparison study is conducted to observe any changes in chemical bond of pineapple leaves after the synthesizing process. Pineapple leaves extract contain numerous bioactive compounds such as glycosides, proteins, phenolics, flavonoids, tannins, and terpenoids. Flavonoids are crucial compounds that act as reducing agents during the synthesis of AgNPs among these compounds. To identify the functional groups that are responsible for capping and stabilizing the Ag nanoparticles, FTIR analysis was performed in the range of 600–4000 cm^{-1} (Marsin and Muhamad, 2020; Emeka et al., 2014). The FTIR spectrum of both sample (A - pineapple leaves extract and B - AgNPs) showed four different peaks (Fig. 6). The stretching intensity shown in the graph of synthesized leaves decreases and becomes broader compare to the control because of the removal of impurities such as hemicellulose and lignin removal (Gnanasekaran et al., 2022). The shifting of peaks between pineapple leaves extract which may suggest the involvement of the functional group in the formation of AgNPs. The presence of hydrogen-bonded hydroxyl (–OH) group compounds was indicated by the broad band at 3,729 cm^{-1} (A) which shifted to 3,735 cm^{-1} (B). The highest energy region of the spectrum, known as the "hydrogen region", ranges from 3,800 to 2,700 cm^{-1} (Baskaran et al., 2016).

The observed peak at 1,610 cm^{-1} (A) which shifted to 1,628 cm^{-1} (B) indicated the presence of C=O stretching bonds of the carbonyl group. Amino acid residues containing carbonyl groups can form a strong bond with metals. Proteins with these residues may create a coating that covers the metal nanoparticles, preventing them from agglomerating in solution. The ligands capping the AgNPs may contain an aromatic compound, C=C of alkenes, or C=N amine stretching, as indicated by previous studies (Baskaran et al., 2016; Jalani et al., 2018). The wide absorption spectra at 1,036 cm^{-1} (A) was due to the stretch vibrations of C-N stretching and C-O stretching of amino and carboxyl groups which mainly attributed from flavonoids and terpenoids in pineapple leaves extract. Then, the reducing of these peaks at 1042 cm^{-1} (B) suggested the involvement of these bioactive compounds in reducing silver ions to AgNPs (Jalani et al., 2018). Therefore, the obtained FTIR spectra provided evidence for the production of AgNPs through the reduction of Ag^{+} ions by the capping material present in the aqueous leaves extract.

3.2.3. XRD analysis

The crystalline phase of the presence and absence of AgNPs sample is analyzed in the range of 2θ between 10° and 100°. As illustrated in Fig. 7, the sample has crystalline structures and three main characteristic peaks at 27.6°, 32° and 46° which are attributed to crystallographic planes at 111, 200 and 220 (crystalline region). These are the crystal reflection planes of the face-centered cubic (fcc) lattice of silver respect to the standard data (Joint Committee on Powder Diffraction Standard data No 04-0783), confirming that the AgNP was successfully green synthesized from wasted pineapple leaves with microwave-assisted treatment. This is validated by previous study as the characteristic peaks were indistinguishable from the biosynthesis of AgNPs from apple pomace (Ren et al., 2019) and aqueous *Desmodium triquetrum* extract (Maryani and Septama, 2022). The observed peaks in this study are also intense and sharp, indicating a high degree of crystallinity of green synthesized AgNPs. Similar patterns are observed for AgNPs synthesized from fern, *Pteris tripartite Sw.* (Baskaran et al., 2016) which showed three intense peaks between 20° and 50°. In comparison of the intensity ratio, crystallographic plane at 200 has the highest intensity. This could be inferred that green synthesized AgNPs is enriched in (200) facets thereby this plane exhibits a preference to align parallel to the surface of the substrate it is supported on, followed by planes at 220 and 111. The crystallite size of AgNPs is calculated using Debye-Scherrer's formula (Krishna et al., 2016):

$$D = 0.94\ \lambda/\beta \cos\theta$$

where D denotes the average crystalline domain size perpendicular to

Table 1
Disk diffusion antibacterial assay of microwave-assisted treatment AgNPs.

Volume of AgNPs with normal treatment (5 mg/mL)	Clear Zone (mm)		
	E. coli	B. subtilis	S. aureus
0 μL (Control)	No clear zone	No clear zone	No clear zone
5 μL	8	8	9
10 μL	9	9	12
Amount of AgNPs with microwave-assisted treatment (5 mg/mL)	Clear Zone (mm)		
	E. coli	B. subtilis	S. aureus
0 μL (Control)	No clear zone	No clear zone	No clear zone
5 μL	9	8	11
10 μL	11	11	14

the reflecting planes, λ denotes the X-ray wavelength, β denotes the full width at half maximum (FWHM), and θ represents the diffraction angle. It is found that the average crystallite domain size of AgNPs was 19 nm which is close to the AgNPs that green synthesized from *Mimosa pudica* leaves extract (Fatimah and Mutiara, 2016).

3.3. Antibacterial activity

3.3.1. Disk diffusion antibacterial assay

Inhibition of three types of bacteria, Gram-negative bacteria *E. coli*, Gram-positive bacteria *B. subtilis* and *S. aureus* (the most common infection bacteria in wound) are summarized in Table 1 and illustrated in Fig. 8. The diameter of inhibitory zone ranges from 8 to 14 mm for normal condition and microwave-assisted treatment AgNPs, respectively. The highest inhibitory effect is observed in the treatment with 10 μL of 5 mg/mL microwave-assisted treatment AgNPs against *S. aureus*, followed by 10 μL of 5 mg/mL normal condition AgNPs against *S. aureus*. It is noticeable that larger inhibitory zones are observed in 10 μL of 5 mg/mL microwave-assisted treatment AgNPs for all types of bacteria as compared to 5 μL of 5 mg/mL normal condition AgNPs. Furthermore, it is noteworthy that both AgNPs perform better antimicrobial activity against *S. aureus* than *E. coli* and *B. subtilis*. Similar observation was reported by Lomelí-Rosales et al. (2022) with green synthesized AgNPs using leaves extract of *Capsicum chinense*. One possible explanation for higher inhibition against *S. aureus* could be owing to the differences in cell membranes and enzymes present in the periplasmic space. The presence of enzymes allows certain Gram-negative bacteria to degrade externally introduced molecules, as described by Duffy and Power (2001). Additionally, the hydrophilic surface of the bacterial outer membrane is high in lipopolysaccharide molecules, which serves as a barrier for antibiotic penetration, adding to their resistance. Conversely, Gram-positive bacteria do not have an outer membrane or even cell wall structure, making them more susceptible to certain antibacterial agents, according to Shan et al. (2007). This is exemplified by the antimicrobial activity of *Vaccinium bracteatum Thunb.* leaves extract where higher inhibition against *S. aureus* than *E. coli* and *B. subtilis* was demonstrated (Zheng et al., 2019).

Additionally, when comparing both Gram-positive bacteria, *S. aureus* exhibits larger inhibitory zones than *B. subtilis*. This difference may be attributed to the non-pathogenic nature of *B. subtilis* in environments. These bacteria even have been explored as potential therapeutic agents of negligible consumer risk (Gonzalez et al., 2011). While *B. subtilis* is generally considered harmless and has reported additional probiotic benefits, the specific mechanism of immune stimulation in the intestinal epithelium is still not well-established scientifically. *B. subtilis* spores are a predominant constituent of probiotic formulae and also available as a stand-alone probiotic (Piewngam and Otto, 2020). These properties could potentially explain the slower formation of inhibitory zone for *B. subtilis* compared to *S. aureus*. However, further detailed studies are necessary to elucidate the underlying mechanism behind this phenomenon.

3.3.2. Broth antibacterial assay

Broth antibacterial assay is also carried out to determine the minimal concentration of AgNPs with microwave-assisted treatment to inhibit the growth of *E. coli*, *B. subtilis*, and *S. aureus*. The control represents the dry cell weight of bacterial growth in nutrient broth without AgNPs. Results in Table 2 shows that the dry cell weight is reducing with the

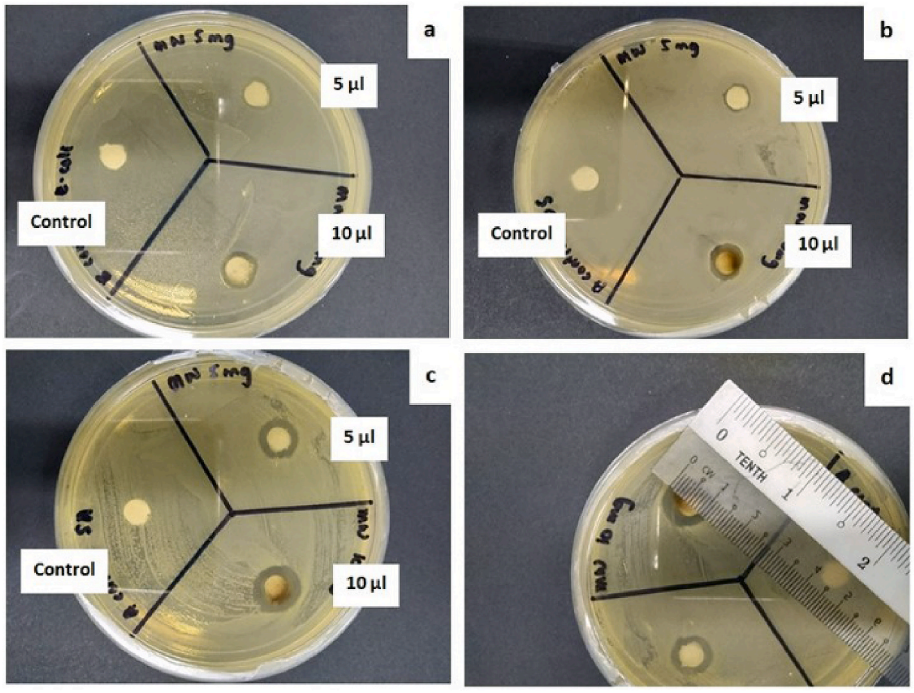

Fig. 8. Measurement of clear zone due to existence of AgNPs on bacteria (a) *E. coli*; (b) *B. subtilis*; (c) *S. aureus* and (d) ruler measurement on the clear zone caused by the AgNPs inhibition activity towards *S. aureus*.

Table 2
Broth antibacterial assay of microwave-assisted treatment AgNPs.

Type of bacteria	AgNPs concentration (μg/mL)	Dry Cell Weight (g/L)
E. coli	0 (control)	0.593 ± 0.013
	20	0.487 ± 0.029
	40	0.057 ± 0.003
	60	0
	80	0
B. subtilis	0 (control)	0.355 ± 0.017
	20	0.503 ± 0.033
	40	0.333 ± 0.015
	60	0
	80	0
S. aureus	0 (control)	1.012 ± 0.036
	20	0.943 ± 0.014
	40	0.086 ± 0.004
	60	0
	80	0

increasing concentration of AgNPs from 20 to 40 μg/mL in the nutrient broth. Moreover, there is no growth determined in the 60 and 80 μg/mL AgNPs samples. This infers that the minimum inhibitory concentration (MIC) of AgNPs for bacterial growth is 60 μg/mL of AgNPs.

There are many possible mechanisms proposed to explain the antimicrobial activity of AgNPs. AgNPs could inhibit the action of microorganism by permeating its peptidoglycan layer, interacting with intracellular components such as DNA, ultimately resulting in cellular damage (Hossain et al., 2019). According to Sathishkumar et al. (2009), the interaction of AgNPs with the -SH groups of proteins on the cell walls could potentially block respiration, leading to cell death. In addition, AgNPs may generate reactive oxygen species (ROS), which cause cellular damage and protein leakage (Ahmed et al., 2018). The biosynthesized AgNPs in this study have a very small size (40–150 nm) and large specific surface area for strong adsorption capacity. Therefore, the antimicrobial activity might perform through the interaction of silver ion on the cell surface by weakening hydrogen bonds (Ren et al., 2019).

4. Conclusion

Green synthesis of AgNPs using microwave-assisted extraction of pineapple (*Ananas comosus*) leaves with $AgNO_3$ solution was successfully demonstrated, which is more economically, environmentally feasible and readily available that could be suitable for rapid production of AgNPs. The use of microwave-assisted treatment with 20 mM $AgNO_3$, 6–8 mL of leaves extract for 2–6 h incubation time has hastened the green synthesis of AgNPs when compared to normal treatment. The presence of the green synthesized AgNPs is confirmed by the results of increasing SPR intensity with increasing incubation time, under UV–Vis spectrophotometry analysis. The hexagonal spherical shape, with a size range between 40 and 150 nm of AgNPs were observed under FE-SEM and has further confirmed the AgNPs biosynthesized using FTIR and XRD analyses. AgNPs also exhibited antimicrobial activity against *E. coli*, *B. subtilis* and *S. aureus* with the minimum inhibitory concentration of silver nanoparticles for bacterial growth is 60 μg/mL. Hence, AgNPs has a potential route for various applications and greater capability to act as an alternative antiseptic agent especially in pharmaceutical industries.

CRediT authorship contribution statement

Siti Nor Syairah Anis: Conceptualization, Investigation, Formal analysis, Writing – original draft, Visualization. **Wen Ching Liew:** Formal analysis, Writing – original draft. **Aishah Mohd Marsin:** Formal analysis, Writing – original draft. **Ida Idayu Muhamad:** Supervision, Writing – review & editing. **Sin Hui Teh:** Investigation, Writing – original draft. **Ahmad Zahran Md Khudzari:** Supervision, Project administration.

Declaration of competing interest

The authors declare that they have no known competing financial interests or personal relationships that could have appeared to influence the work reported in this paper.

Data availability

The data that has been used is confidential.

Acknowledgement

We express our gratitude for the funding received from the Malaysia Ministry of Higher Education and Universiti Teknologi Malaysia. The financial support was provided through the Malaysia Research University Network (MRUN), with grant number UPM/800-4/11/MRUN/2019/5539160. We would also like to extend our appreciation to the Food and Biomaterial Engineering Research Group (FoBERG) and the Department of Bioprocess and Polymer Engineering for their invaluable support.

References

Acharya, D., Singha, K.M., Pandey, P., Mohanta, B., Rajkumari, J., Singha, L.P., 2018. Shape dependent physical mutilation and lethal effects of silver nanoparticles on bacteria. Sci. Rep. 8 (1), 1–11. https://doi.org/10.1038/s41598-017-18590-6.

Ahmed, B., Hashmi, A., Khan, M.S., Musarrat, J., 2018. ROS mediated destruction of cell membrane, growth and biofilms of human bacterial pathogens by stable metallic AgNPs functionalized from bell pepper extract and quercetin. Adv. Powder Technol. 29 (7), 1601–1616. https://doi.org/10.1016/j.apt.2018.03.025.

Ahmed, S., Ahmad, M., Swami, B.L., Ikram, S., 2016. A review on plants extract mediated synthesis of silver nanoparticles for antimicrobial applications: a green expertise. J. Adv. Res. 7 (1), 17–28.

Al-Askar, A.A., Hafez, E.E., Kabeil, S.A., Meghad, A., 2013. Bioproduction of silver-nano particles by Fusarium oxysporum and their antimicrobial activity against some plant pathogenic bacteria and fungi. Life Sci. J. 10 (3), 2470–2475.

Alsamhary, K.I., 2020. Eco-friendly synthesis of silver nanoparticles by Bacillus subtilis and their antibacterial activity. Saudi J. Biol. Sci. 27 (8), 2185–2191.

Arshad, H., Sami, M.A., Sadaf, S., Hassan, U., 2021. Salvadora persica mediated synthesis of silver nanoparticles and their antimicrobial efficacy. Sci. Rep. 11 (1), 1–11. https://doi.org/10.1038/s41598-021-85584-w.

Baskaran, X., Vigila, A.V.G., Parimelazhagan, T., Muralidhara-Rao, D., Zhang, S., 2016. Biosynthesis, characterization, and evaluation of bioactivities of leaf extract-mediated biocompatible silver nanoparticles from an early tracheophyte, Pteris tripartita Sw. Int. J. Nanomed. 11, 5789. https://doi.org/10.2147/IJN.S108208.

Chawalitsakunchai, W., Dittanet, P., Loykulnant, S., Sae-oui, P., Tanpichai, S., Seubsai, A., Prapainainar, P., 2021. Properties of natural rubber reinforced with nano cellulose from pineapple leaf agricultural waste. Mater. Today Commun. 28, 102594 https://doi.org/10.1016/j.mtcomm.2021.102594.

Duffy, C.F., Power, R.F., 2001. Antioxidant and antimicrobial properties of some Chinese plant extracts. Int. J. Antimicrob. Agents 17 (6), 527–530.

Emeka, E.E., Ojiefoh, O.C., Aleruchi, C., Hassan, L.A., Christiana, O.M., Rebecca, M., Dare, E.O., Temitope, A.E., 2014. Evaluation of antibacterial activities of silver nanoparticles green-synthesized using pineapple leaf (*Ananas comosus*). Micron 57, 1–5. https://doi.org/10.1016/j.micron.2013.09.003.

Fatimah, I., Mutiara, N.A.L., 2016. Biosynthesis of silver nanoparticles using Putri Malu (Mimosa pudica) leaves extract and microwave irradiation method. Molekul 11 (2), 288–298. https://doi.org/10.20884/1.jm.2016.11.2.221.

Galatage, S.T., Hebalkar, A.S., Dhobale, S.V., Mali, O.R., Kumbhar, P.S., Nikade, S.V., Killedar, S.G., 2021. Silver nanoparticles: properties, synthesis, characterization, applications and future trends. Silver micro-nanoparticles-properties, synthesis, characterization, and applications. https://doi.org/10.5772/intechopen.99173.

Gnanasekaran, S., Nordin, N.I.A.A., Jamari, S.S., Shariffuddin, J.H., 2022. Effect of Steam-Alkaline coupled treatment on N36 cultivar pineapple leave fibre for isolation of cellulose. Mater. Today: Proc. 48, 753–760. https://doi.org/10.1016/j.matpr.2021.02.216.

Gonzalez, D.J., Haste, N.M., Hollands, A., Fleming, T.C., Hamby, M., Pogliano, K., Nizet, V., Dorrestein, P.C., 2011. Microbial competition between Bacillus subtilis and Staphylococcus aureus monitored by imaging mass spectrometry. Microbiology 157 (9), 2485–2492. https://doi.org/10.1099/mic.0.048736-0.

Hamdiani, S., Shih, Y.F., 2021. A green method for synthesis of silver-nanoparticles-diatomite (AgNPs-D) composite from pineapple (*Ananas comosus*) leaf extract. Indonesian Journal of Chemistry 21 (3), 740–752. https://doi.org/10.22146/ijc.63573.

Hossain, M.M., Polash, S.A., Takikawa, M., Shubhra, R.D., Saha, T., Islam, Z., et al., 2019. Investigation of the antibacterial activity and in vivo cytotoxicity of biogenic silver nanoparticles as potent therapeutics. Front. Bioeng. Biotechnol. 7, 239. https://doi.org/10.3389/fbioe.2019.00239.

Jalani, N.S., Michell, W., Lin, W.E., Hanani, S.Z., Hashim, U., Abdullah, R., 2018. Biosynthesis of silver nanoparticles using Citrus grandis peel extract. Malaysian Journal of Analytical Sciences 22 (4), 676–683.

Jyothi, D., Priya, S., James, J.P., 2022. MICROWAVE-ASSISTED green synthesis of silver nanoparticles using extract of spondias pinnata bark. J. Microbiol. Biotechnol. Food Sci. 12 (3), e1951 https://doi.org/10.55251/jmbfs.1951.

Kaur, N., Singh, A., Ahmad, W., 2022. Microwave assisted green synthesis of silver nanoparticles and its application: a review. J. Inorg. Organomet. Polym. https://doi.org/10.1007/s10904-022-02470-2.

Krishna, A.G., Ravikumar, R.V.S.S.N., Kumar, T.V., Ephraim, S.D., Ranjith, B., Pranoy, M., Dola, S., 2016. Investigation and comparison of optical and Raman bands of mechanically synthesised MoO 3 Nano powders. Mater. Today: Proc. 3 (1), 54–63. https://doi.org/10.1016/j.matpr.2016.01.121.

Krishnaraj, C., Jagan, E.G., Rajasekar, S., Selvakumar, P., Kalaichelvan, P.T., Mohan, N. J., 2010. Synthesis of silver nanoparticles using Acalypha indica leaf extracts and its antibacterial activity against water borne pathogens. C. S. B. B Colloids Surf. B Biointerfaces 76 (1), 50–56. https://doi.org/10.1016/j.colsurfb.2009.10.008.

Kumar, M.A., Sonal, U., Akshi, G., Kumar Ebenezer, J., Lawrence, R., Nidhi, M., 2021. Microwave assisted green synthesis of silver nanoparticles with leaf of Ficus racemosa and its in vitro antibacterial analysis and dye catalytic activity. Res J Chem Environ 25, 111–119.

Lade, B., Patil, A., 2022. Green synthesis and characterization of silver nanoparticles synthesized using leaf extract of Passiflora foetida Linn. Journal of Sustainable Materials Processing and Management 2 (2), 57–68. https://doi.org/10.30880/jsmpm.2022.02.02.008.

Lin, P., Moore, D., Allhoff, F., 2009. What is Nanotechnology and Why Does it Matter?: from Science to Ethics. John Wiley & Sons.

Lomelí-Rosales, D.A., Zamudio-Ojeda, A., Reyes-Maldonado, O.K., López-Reyes, M.E., Basulto-Padilla, G.C., Lopez-Naranjo, E.J., et al., 2022. Green synthesis of gold and silver nanoparticles using leaf extract of Capsicum chinense plant. Molecules 27 (5), 1692. https://doi.org/10.3390/molecules27051692.

Madkour, L.H., 2019. Introduction to nanotechnology (NT) and nanomaterials (NMs). In: Nanoelectronic Materials. Advanced Structured Materials, vol. 116. Springer, Cham. https://doi.org/10.1007/978-3-030-21621-4_1.

Marsin, A.M., Muhamad, I.I., 2020. Application of box-behnken design with response surface methodology for optimizing oxygen colour indicator for active packaging. Malaysian Journal of Analytical Sciences 24 (1), 42–52.

Maryani, F., Septama, A.W., 2022. Microwave-assisted green synthesis of Desmodium triquetrum-mediated silver nanoparticles: enhanced antibacterial, antibiofilm, and cytotoxicity activities against human breast cancer cell lines. Materials Advances 3 (22), 8267–8275. https://doi.org/10.1039/d2ma00613h.

Mojally, M., Sharmin, E., Obaid, N.A., Alhindi, Y., Abdalla, A.N., 2022. Polyvinyl alcohol/corn starch/castor oil hydrogel films, loaded with silver nanoparticles biosynthesized in Mentha piperita leaves' extract. J. King Saud Univ. Sci. 34 (4), 101879 https://doi.org/10.1016/j.jksus.2022.101879.

Nagalingam, M., Kalpana, V.N., Panneerselvam, A., 2018. Biosynthesis, characterization, and evaluation of bioactivities of leaf extract-mediated biocompatible gold nanoparticles from Alternanthera bettzickiana. Biotechnology Reports 19, e00268. https://doi.org/10.1016/j.btre.2018.e00268.

Nithya, D.K.A., Vimala, R., 2014. Biosynthesis of Silver Nanoparticles Using *Aegle Marmelos* (Bael) Fruit Extract and its Application to Prevent Adhesion of Bacteria: A Strategy to Control Microfouling, vol. 2014. Bioinorganic Chemistry and Applications. https://doi.org/10.1155/2014/949538. Article ID 949538, 8 pages.

Piewngam, P., Otto, M., 2020. Probiotics to prevent Staphylococcus aureus disease? Gut Microb. 11 (1), 94–101. https://doi.org/10.1080/19490976.2019.1591137.

Priyadarshini, S., Gopinath, V., Priyadharsshini, N.M., MubarakAli, D., Velusamy, P., 2013. Synthesis of anisotropic silver nanoparticles using novel strain, Bacillus flexus and its biomedical application. Colloids Surf. B Biointerfaces 102, 232–237. https://doi.org/10.1016/j.colsurfb.2012.08.018.

Ramya, E., 2021. Green synthesis of metal nanostructures and its nonlinear optical properties. In: Nonlinear Optics-Nonlinear Nanophotonics and Novel Materials for Nonlinear Optics. IntechOpen.

Ren, Y.Y., Yang, H., Wang, T., Wang, C., 2019. Bio-synthesis of silver nanoparticles with antibacterial activity. Mater. Chem. Phys. 235, 121746 https://doi.org/10.1016/j.matchemphys.2019.121746.

Sabbagh, F., Kiarostami, K., Khatir, N.M., Rezania, S., Muhamad, I.I., Hosseini, F., 2021. Effect of zinc content on structural, functional, morphological, and thermal properties of kappa-carrageenan/NaCMC nanocomposites. Journal of Polymer Testing 93, 106922. https://doi.org/10.1016/j.polymertesting.2020.106922.

Salari, S., Bahabadi, S.E., Samzadeh-Kermani, A., Yosefzaei, F., 2019. In-vitro evaluation of antioxidant and antibacterial potential of green synthesized silver nanoparticles using Prosopis farcta fruit extract. Iran. J. Pharm. Res. (IJPR): IJPR 18 (1), 430.

Sathishkumar, M., Sneha, K., Won, S.W., Cho, C.W., Kim, S., Yun, Y.S., 2009. Cinnamon zeylanicum bark extract and powder mediated green synthesis of nano-crystalline silver particles and its bactericidal activity. Colloids Surf. B Biointerfaces 73 (2), 332–338. https://doi.org/10.1016/j.colsurfb.2009.06.005.

Shan, B., Cai, Y.Z., Brooks, J.D., Corke, H., 2007. The in vitro antibacterial activity of dietary spice and medicinal herb extracts. Int. J. Food Microbiol. 117 (1), 112–119.

Wang, E.C., Wang, A.Z., 2014. Nanoparticles and their applications in cell and molecular biology. Integr. Biol. 6 (1), 9–26. https://doi.org/10.1039/c3ib40165k.

Zheng, Y., Chen, L., Liu, Y., Shi, L., Wan, S., Wang, L., 2019. Evaluation of antimicrobial activity of water-soluble flavonoids extract from Vaccinium bracteatum Thunb. leaves. Food Sci. Biotechnol. 28, 1853–1859. https://doi.org/10.1007/s10068-019-00634-4, 9.